Journal of Power Sources 184 (2008) 675–681

Contents lists available at ScienceDirect

Journal of Power Sources

journal homepage: www.elsevier.com/locate/jpowsour

# Influence of high temperature treatment of porous carbon on the electrochemical performance in supercapacitor

Yongming Tian[a,b], Yan Song[a,*], Zhihong Tang[a,b], Quangui Guo[a], Lang Liu[a]

[a] Key Laboratory of Carbon Materials, Institute of Coal Chemistry, Chinese Academy of Sciences, 27th South Taoyuan Road, Taiyuan City, Shanxi Province 030001, China
[b] Graduate University of Chinese Academy of Sciences, China

ARTICLE INFO

*Article history:*
Received 7 January 2008
Received in revised form 27 April 2008
Accepted 28 April 2008
Available online 4 May 2008

*Keywords:*
Supercapacitor
High temperature treatment
Electrical conductivity
IR drop
Equivalent series resistance

ABSTRACT

Mesoporous carbon (MoC), prepared by the template method from phenol resin, commercial mesoporous carbon fiber (ACF) and microporous activated carbon (MiC) were heat-treated under 1200 °C in nitrogen. The samples before and after high temperature heat treatment (HTT) were used as electrodes in 30% KOH electrolyte for supercapacitor. The structure and electrochemical properties of these samples were characterized by X-ray diffraction (XRD), galvanotactic charge–discharge, cyclic voltammetry (CV) and electrochemical impedance spectra, respectively. Results showed that HTT caused a remarkable increase of mesoporous ratio in texture accompanied with a significant reduction of surface area. After HTT, the layer–layer space among graphite crystallite decreased and the degree of graphitization was improved. The capacitance values of mesoporous carbons increased and a more stable tendency for specific capacitance was obtained compared with the contrary performance of MiC-1200. The cyclic voltammetry of the samples at different sweep rates was close to the rectangular shape, which represented the lower ESR and higher power density. It was also found that high temperature treatment could improve the electrical conductivity and decrease the impedance of the electrode remarkably. The improved specific capacitance and the better conductivity of mesoporous carbons could be ascribed to the expanding and reorganization of crystallite structure as well as increase of mesopore ratio.



## 1. Introduction

As a potential alternative or complement to other energy storage or generation devices such as secondary batteries and fuel cells, the research and development of supercapacitor had attracted much attention [1–5]. Carbon materials were thought to be the most attractive electrode materials because of its excellent electrochemical property, high surface area, relatively low cost and availability [6–8]. In particular, mesoporous carbon obtained by template method of phenol resin-derived precursors generally exhibited very good electrochemical performance in this application. In the carbon-based supercapacitor, energy was stored mainly through the formation of the electrical double layer, as a result, the structure and property of the carbon electrode will greatly influence the performance of the as-prepared supercapacitor. Beguin et al. had revealed that lower equivalent series resistance might lead to higher power density of supercapacitor [9], which was mainly attributed to the improvement of crystallite structure. As a result, improving the conductivity of the porous carbon material could enhance the performance of the supercapacitor.

It is well known that carbon with higher graphitization and better crystallite structure had the better conductivity and high temperature treatment was an effective way to accelerate the formation of the crystallite structure of graphite and improved the degree of graphitization [10]. Ruiz et al. studied the effects of thermal treatment on activated carbon at 600 and 1000 °C [11]. The results showed that the presence of an extra capacitance due to redox reactions had been proved for the samples with high oxygen content. However, other factors, such as conductivity or wettability, which also influenced the total capacitance and were certainly modified by the thermal treatment, were not taken into account in their work.

In this paper, several kinds of porous carbons, including microporous carbon (MiC) and mesoporous cabon/fiber (MoC and ACF), were treated at 1200 °C in nitrogen, and then used as electrodes in 30% KOH electrolyte for supercapacitor. The relationship between structure and the electrochemical performance of these samples were investigated.

* Corresponding author. Tel.: +86 351 4250553; fax: +86 351 4083952.
*E-mail address:* yansong1026@126.com (Y. Song).

0378-7753/$ – see front matter. 
doi:10.1016/j.jpowsour.2008.04.070

**Table 1**
Porous structure of samples

| | MiC | MiC-1200 | MoC | MoC-1200 | ACF | ACF-1200 |
|---|---|---|---|---|---|---|
| $S_{BET}$ ($m^2\,g^{-1}$) | 2962 | 2001 | 607 | 269 | 1195 | 1021 |
| $V_{total}$ ($cm^3\,g^{-1}$) | 0.8 | 0.54 | 0.67 | 0.52 | 0.94 | 1.09 |
| $V_{micro}$ ($cm^3\,g^{-1}$) | 0.74 | 0.46 | 0.09 | 0.01 | 0.29 | 0.27 |
| $V_{meso}$ ($cm^3\,g^{-1}$) | 0.06 | 0.08 | 0.58 | 0.51 | 0.65 | 0.82 |
| %meso | 7.5 | 14.8 | 86.6 | 97.7 | 69.1 | 75.2 |

*Remark*: $S_{BET}$, specific surface area ($m^2\,g^{-1}$); $V_{total}$, total pore volume ($cm^3\,g^{-1}$); $V_{micro}$, micropore volume ($cm^3\,g^{-1}$); $V_{meso}$, mesopore volume ($cm^3\,g^{-1}$); %meso, mesoporosity percentage after HTT.

## 2. Experimental

### 2.1. Materials

Mesoporous carbon was prepared by the template method [12], commercial ACF and activated carbon (MiC) was purchased from Osaka Gas Company and Hua Xian Activated Carbon Company. The porous carbons were thermally treated at 1200 °C in a horizontal furnace under a nitrogen flow of 65 mL $s^{-1}$ for an hour, and then cooled to room temperature. The resultant samples after heat treatment were labeled as MoC-1200, ACF-1200 and MiC-1200, respectively. Pore structure and pore size distribution of all the samples were shown in Table 1 and Fig. 1.

### 2.2. Characterization

Porous texture of samples was characterized by nitrogen adsorption at 77 K using Micromeritics ASAP-2010 instrument. The pore size distribution curve of MiC and ACF series were calculated by the density functional theory (DFT) method, while that of mesoporous carbon MoC series were calculated by the BJH method. The specific surface areas ($S_{BET}$) were calculated from the adsorption data in the relative pressure interval from 0.04 to 0.2 using the Brunauer–Emmett–Teller (BET) method. The total pore volume ($V_{total}$) was calculated at relative pressure of 0.99. The micropore volume ($V_{micro}$) was determined by t-plot model, and the mesopore volume ($V_{meso}$) was calculated by the difference of $V_{total}$ and $V_{micro}$. The ratio of mesopore (%meso) was obtained from the ratio of $V_{meso}$ and $V_{total}$.

The X-ray diffraction (XRD) analysis was performed in using the Bruker D8-Advamce Instrument (Germany), which was analyzed on a bed diffractometer over a $2\theta$ range of 23–80° using Cu Kα radiation as the light source with the tube potential of 40 kV and tube current of 40 mA.

The sheet-type electrodes about 400–500 μm in thickness and 12 mm in diameter were prepared by mixing porous carbon (80 mass%) and graphite (10 mass%) with polytetrafluoroethylene (PTFE) binder (10 mass%) followed by kneading and rolling to a thin sheet. A polypropylene separator with the thickness of 40 μm was sandwiched with a pair of the sample sheets to form electrodes. The capacitance of the sample electrode was determined by two electrodes system without reference electrode. 30% KOH was employed as electrolyte. The charge/discharge capacitance of electrode was measured using a Program Testing System (produced by Wuhan Lixing Co. Ltd., China). Charge and discharge voltages were ranged

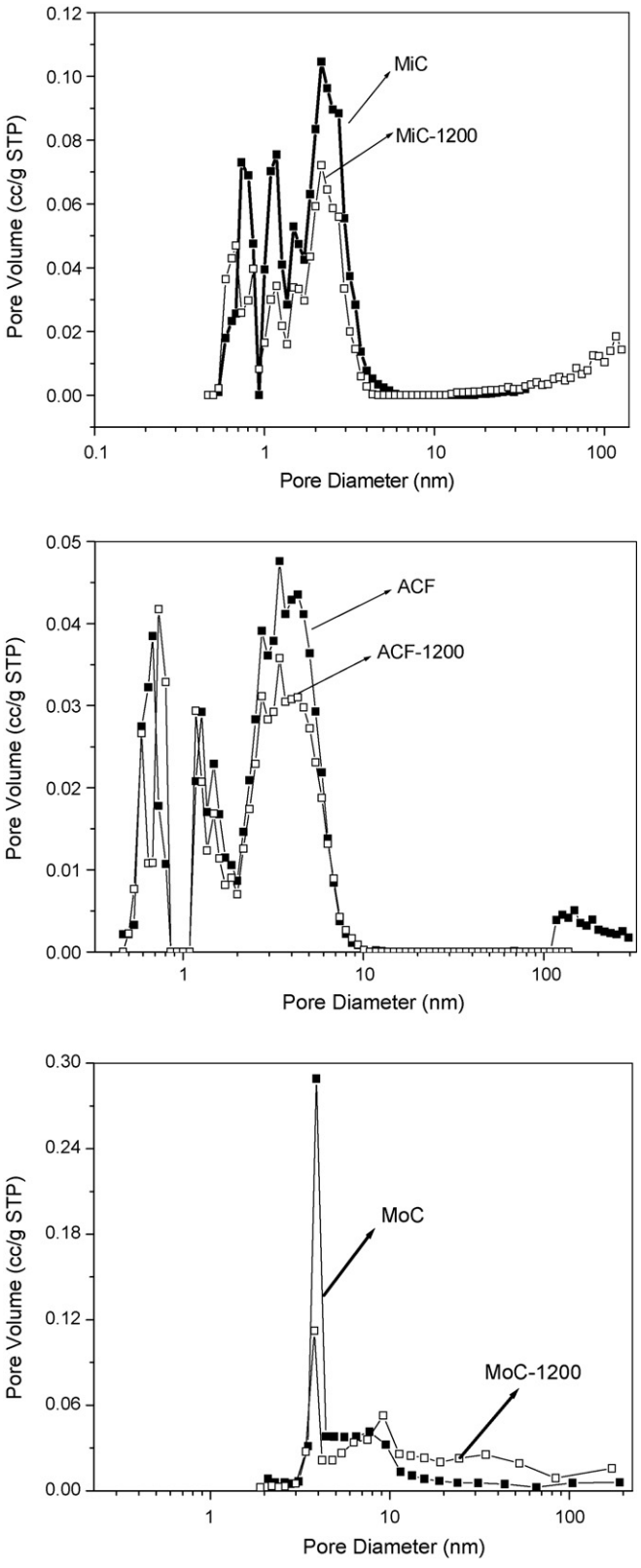


**Fig. 1.** Pore structure distribution of (a) MiC and MiC-1200; (b) ACF and ACF-1200; (c) MoC and MoC-1200.

**Table 2**
Specific capacitance of samples at 0.5 mA

| | MiC | MiC-1200 | MoC | MoC-1200 | ACF | ACF-1200 |
|---|---|---|---|---|---|---|
| $C_g$ ($F\,g^{-1}$) | 209.1 | 192.8 | 88.3 | 75.7 | 131.2 | 118.9 |
| $C$ ($\mu F\,cm^{-2}$) | 0.10 | 0.07 | 0.15 | 0.27 | 0.11 | 0.12 |

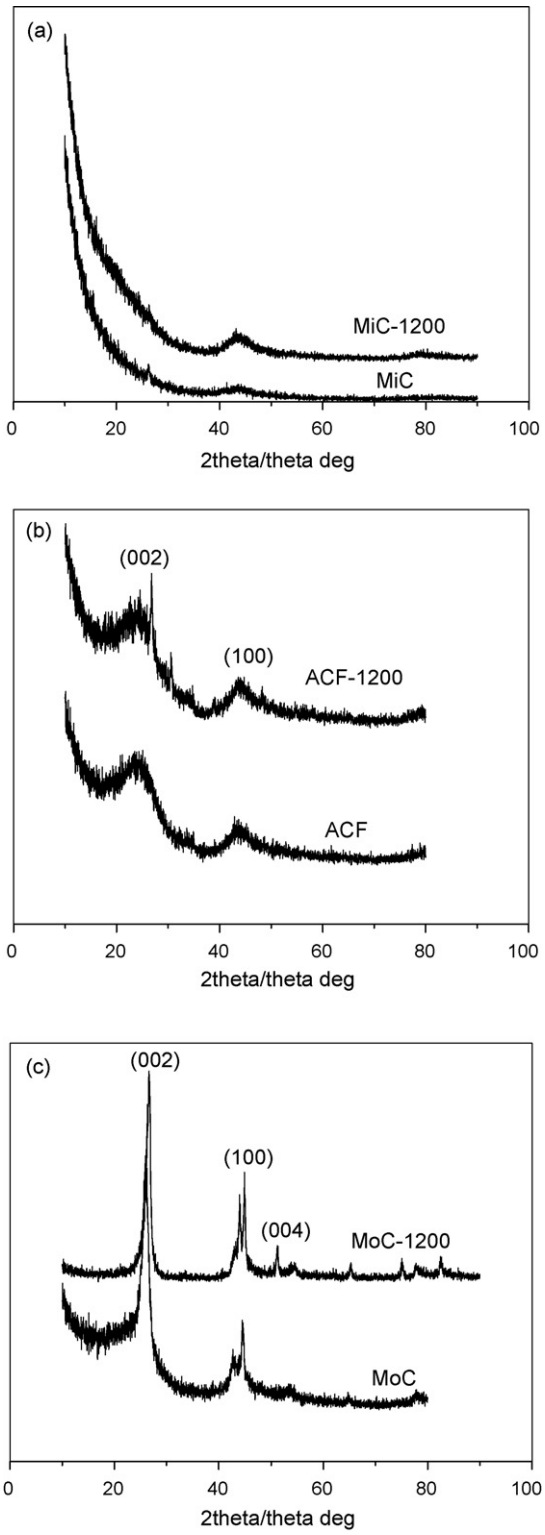


**Fig. 2.** XRD profile of (a) MiC and MiC-1200; (b) ACF and ACF-1200; (c) MoC and MoC-1200.

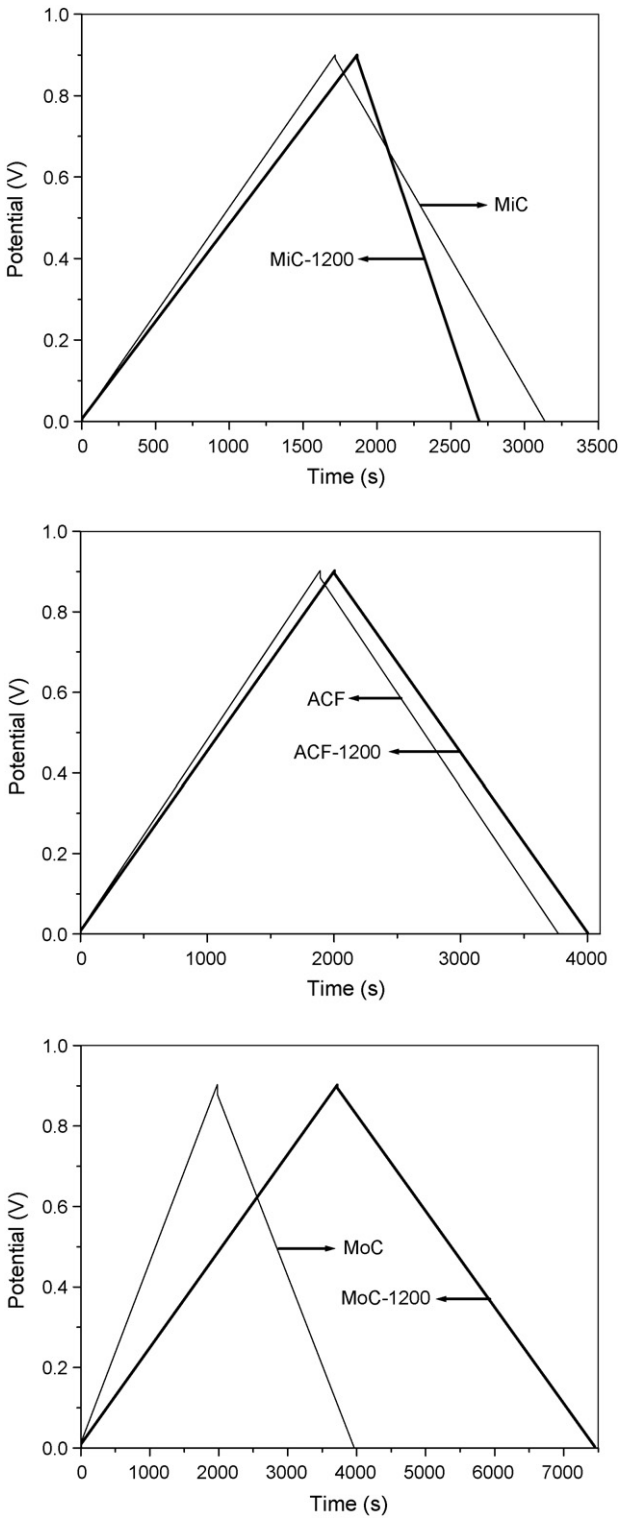


**Fig. 3.** Constant current charge/discharge curve of samples (0.5 mA).

between 0.9 and 0 V. The C in Farad was calculated on the basis of:

$$C = \left[\frac{i\,(\mathrm{A}) \times t\,(\mathrm{s})}{W\,(\mathrm{g}) \times \Delta E\,(\mathrm{V})}\right] \quad (1)$$

where $i$ is the discharge current, which is chosen as constant for all the samples, $t$, the discharge time, $W$, the mass of the active carbon material of the single electrode (working electrode), and $\Delta E$ is the potential difference during discharge. For each sample, at least three electrodes were assembled and measured as parallel experiment. The specific capacitance $C_g$ was expressed as $\mathrm{F\,g^{-1}}$ of carbon electrode material. The surface capacitance $C\,(\mu\mathrm{F\,cm^{-2}})$ was defined as the gravimetric specific capacitance $(\mathrm{F\,g^{-1}})$ divided by BET surface area.

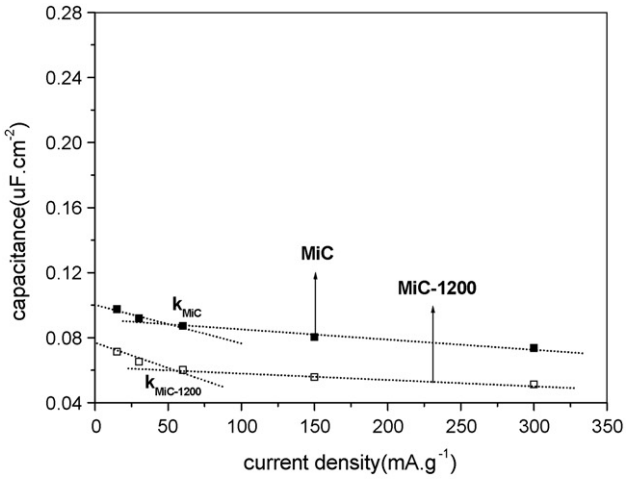


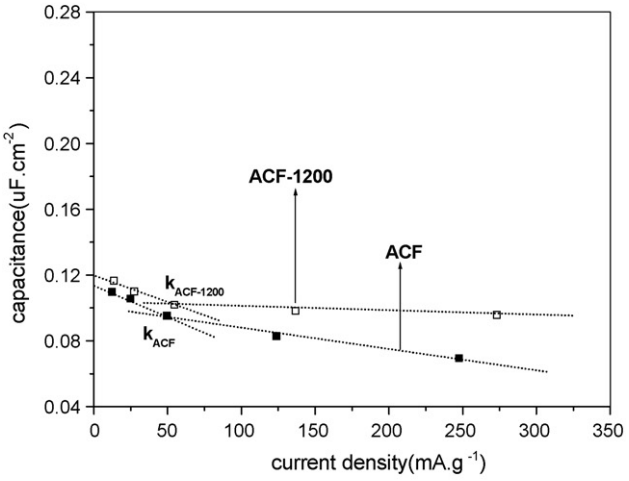


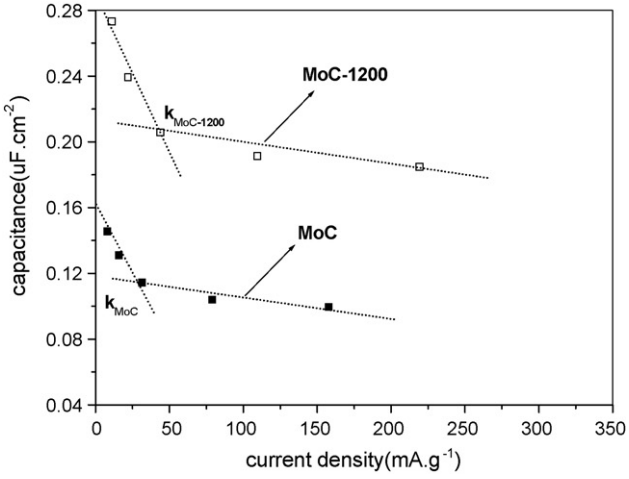


**Fig. 4.** Variation of specific capacitance with current density (*k* means the intersection of every two straight lines).

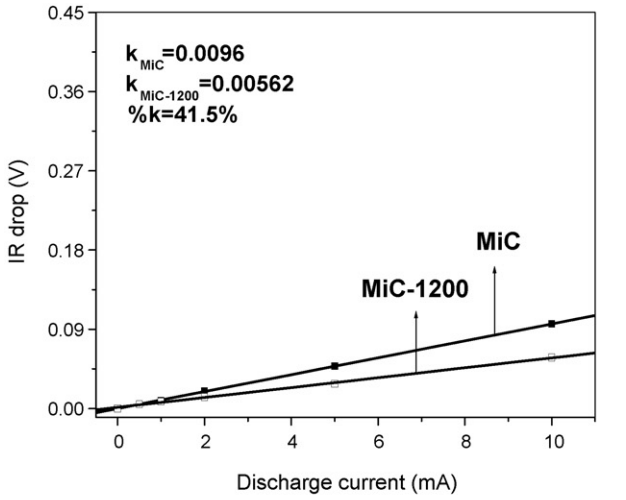


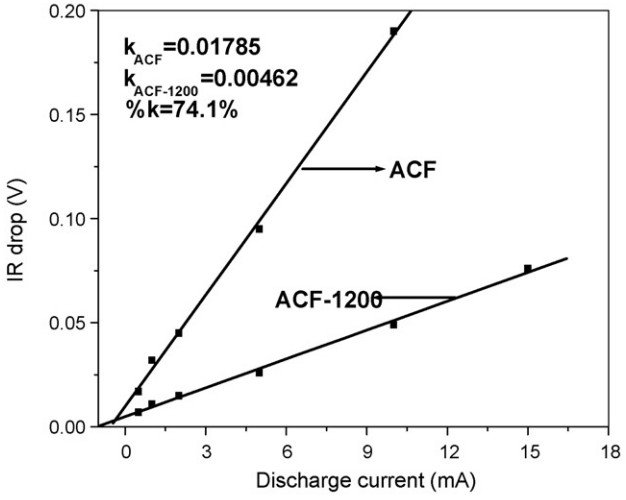


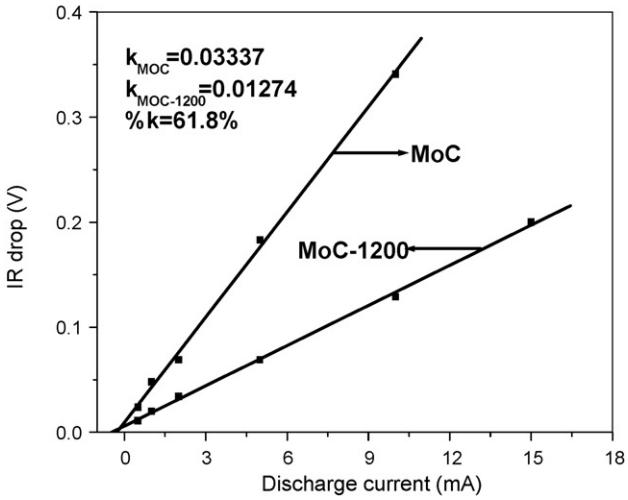


**Fig. 5.** Variation of IR drop with discharge current for all the samples (*k* means the slope of straight line; %*k* means the decreasing scope of *k* after HTT).

CHI660C Instrument (produced by Shanghai Chenhua Co. Ltd., China) was used to measure the electrochemical impedance spectra (EIS) and cyclic voltammetry (CV) of the electrodes. The EIS measurements were carried out in the frequency range from 100 kHz to 0.01 Hz and the scanning rate altered from 0.01 to 0.1 V $s^{-1}$.

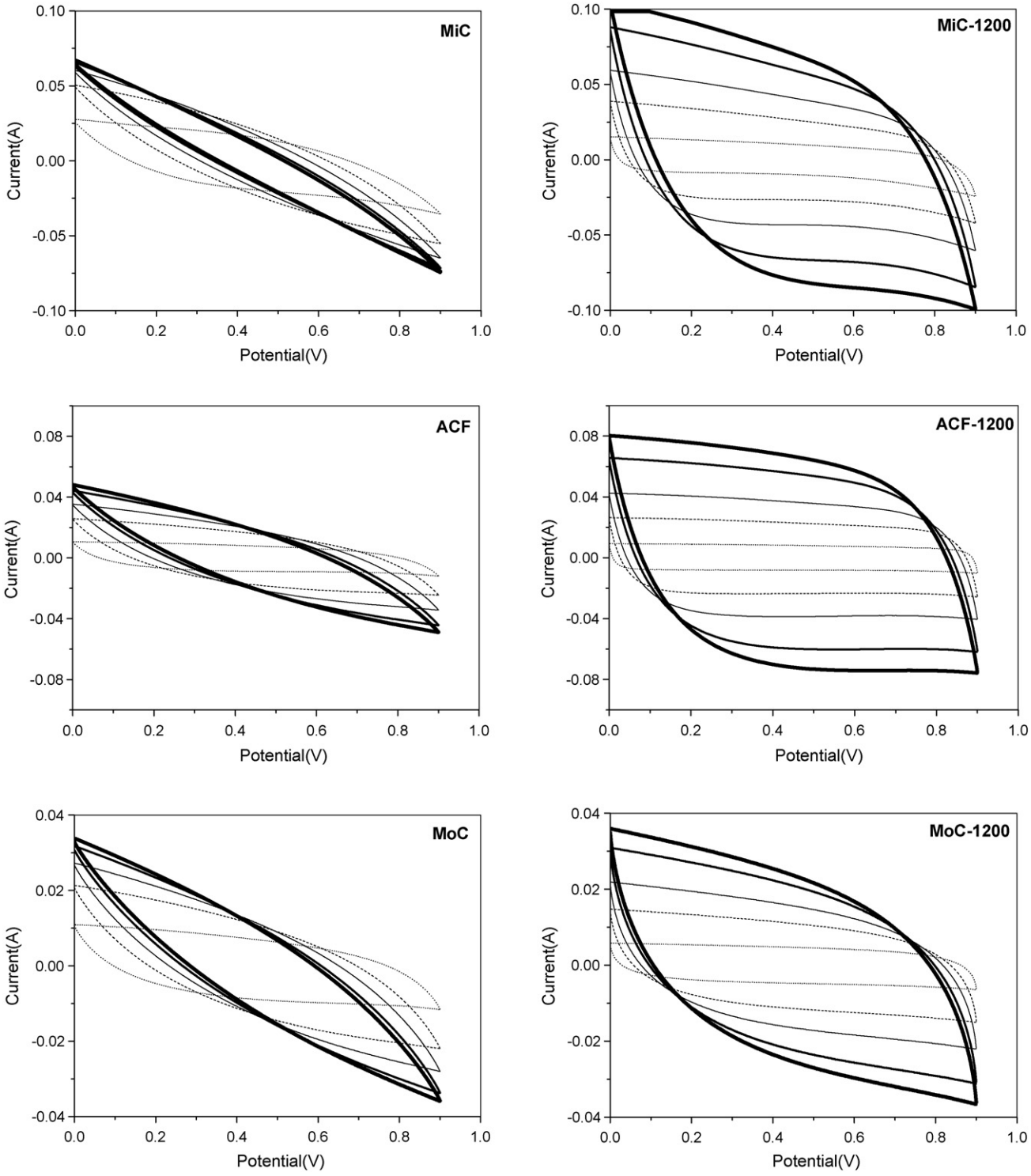


**Fig. 6.** Cyclic voltammetry of all the porous carbon samples in different sweep rate (sweep rate: (. . .) 0.01 V $s^{-1}$, (- - -) 3 V $s^{-1}$, (—) 0.05 V $s^{-1}$, (▬) 0.08 V $s^{-1}$ and (▬) 0.1 V $s^{-1}$).

## 3. Results and discussion

### 3.1. Structure of porous carbons

The pore size distributions and the pore structure parameters before and after higher temperature treatment of the samples was shown in Fig. 1 and Table 1. It can be seen that for the samples before higher temperature treatment, MiC contained pores mainly below 2 nm, ACF contained not only micropores below 2 nm but also mesopores at about 3.4 nm, while MoC possessed mesopores at about 4 nm. Among these three samples, MoC had the highest mesopore ratio of about 86.6%, and MiC possessed the least mesopore ratio of about 7.5%. The order of the surface area of the sample was as following: MiC > ACF > MoC. After high temperature treatment (HTT), the surface area of all the samples decreased (as shown in Table 1), and the drastic decrease was observed for MoC. How-

ever, the pore size distributions changed a little in spite of reducing in pore volumes of the samples (Fig. 1).

Liu et al. [13] found that HTT would cause the significant decrease of total pore volume as well as surface area, which ascribed to the expanding and reorganization of crystallite structure of porous carbon. Fig. 2 shows the comparison of XRD spectrum for these samples. The peaks at 26.3°, 43.75° and 54.70° could be assigned to the diffraction of (0 0 2), (1 0 0) and (0 0 4) plane of the carbon [14,15], respectively, which were proportional to the crystal size, e.g. the height of (0 0 2) peak was proportional to $L_c$ and the height of (1 0 0) peak was proportional to $L_a$. As seen from Fig. 2, for MiC and MiC-1200, $L_c$ were similar, while the $L_a$ size of MiC-1200 changed slightly. However, for MoC, both $L_a$ and $L_c$ values changed greatly after HTT. The stronger and sharper diffraction peak of which, at 26.3°, suggests that the products were well crystallized. This fact indicated that HTT had more significant influence on the crystallite structure of MoC. For ACF, the structural change after HTT was between that of MiC and MoC, and the peak intensity at 26.3° and 43.75° tended to be more obvious.

### 3.2. Electrochemical characteristic

Fig. 3 shows the charge–discharge curves obtained from the different samples at 0.5 mA, which were used to calculate the surface capacitance $C$ ($\mu F\,cm^{-2}$), as shown in Table 2. It can be seen that mesoporous carbons (MoC and ACF) showed better specific capacitance than microporous MiC. After HTT, the specific capacitance of mesoporous carbons (MoC and ACF) increased, especially for MoC-1200 (the specific capacitance increased up to as high as twice of MoC), while the specific capacitance of microporous MiC-1200 decreased to some extent. Influence of current density on the specific capacitance determined for the three samples was shown in Fig. 4. It was found that for all three samples, the capacitance reduced with the increase of current density. Mesoporous carbons (MoC and ACF) before or after HTT always showed much higher capacitance than that of microporous carbon (MiC) in the same current density. The gradient of all the curves after HTT was less steep with the increase of current density and tended to be horizontal especially for that of mesoporous carbons, here $k$ was used to show the dramatic inflexion. From the estimate of gradient for all the samples, HTT had the clearest improvement to mesoporous ACF (increasing rate of slope being 78.5%).

The IR drop against the discharge current was plotted in Fig. 5. This potential drop mainly originated from the bulk solution resistance, electrode resistance, and ion migration resistance in the electrode [16,17]. The slope of the linear relationship between the IR drop and discharge current could be used to estimate the overall resistance of the capacitors, $k$ and $\%k$ were used to express the slope of straight and decreasing percentage of $k$ after HTT, respectively. With the increase of current density, incomplete discharge appeared among the as-formed electric doubly layers, so IR drop enhanced in the beginning of discharge. As could be seen in Fig. 5, the value of $\%k$ could easily be calculated as the order 41.5%, 61.8% and 74.1% for MiC, MoC and ACF, respectively, which indicated the conductivity of ACF-1200 had the most prominent improvement. That is to say, HTT improved the conductivity and reduced the overall resistance effectively especially for mesoporous carbon/fiber.

The CV with different sweep rates for all the samples were shown in Fig. 6. The inner integrated area of CV curve of samples, which stands for the power density, increased and the slope of $V/I$, which stands for equivalent series resistance (ESR), decreased after HTT. For mesoporous carbon/fiber, the CV curves of MoC-1200 (especially in the lowest sweep rate) and ACF-1200 (even in the highest sweep rate) were close to rectangular shape, indicating the smallest ESR in the mesoporous carbon samples. With the increase of sweep rate, the inner integrated area increased, which represented the higher charge/discharge rate and better power density subsequently.

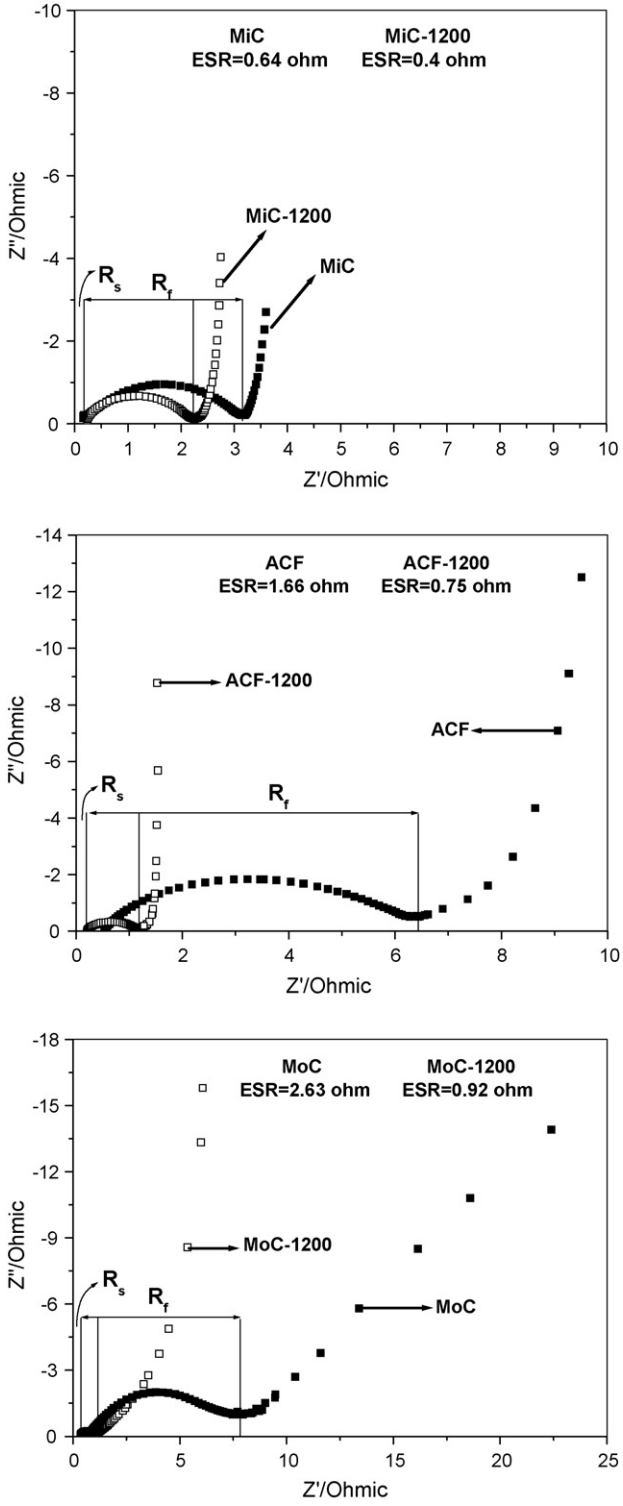


**Fig. 7.** Nyquist plot of all the porous carbon samples (100 kHz to 0.01 Hz).

In order to understand the impedance performance clearly, Nyquist plot of all the porous carbon samples were shown in Fig. 7. The electrolyte resistance [18], $R_s$, was constant but varies with electrolyte. $R_f$ represented the sum of the resistance of the electrode itself and the contact resistance between the electrode and

the current collector. The electrolyte resistance and the contact resistance were identical in all samples. Therefore, a decrease of $R_f$ indicated a decrease of the porous carbon resistance. The ideally polarizable capacitance would give rise to a straight line along the imaginary axis ($Z''$). In a real capacitor with series resistance, this line had a finite slope, representing the diffusive resistivity of the electrolyte within the pore of the electrode. Fig. 7 revealed that the order of $R_f$ was as follows: MiC < ACF < MoC, which meant that MiC had the lowest resistance, and MoC possessed highest resistance. After HTT, the diffusive line of the samples came close to an ideally straight line, especially for MoC-1200 and ACF-1200. ESR values of these samples were also listed in Fig. 7. It can be found that the ESR of all samples decreased after HTT, and the decrease extent was different (37.5% for MiC, 54.8% for ACF and 65% for MoC, respectively) As stated above, HTT would cause a clear increase of mesopore ratio, expanding and reorganization of crystallite structure of porous carbon. The more regular crystallite structure and higher mesopore ratio of mesoporous carbons after thermal treatment not only brought about the higher double layer capacitance, as well as the smooth charge–discharge performance in high current density, but also effectively decreased the ESR for porous carbons [13,19].

## 4. Conclusions

High temperature treatment of porous carbons at 1200 °C caused a clear increase of mesoporous ratio in texture accompanied with a significant reduction of surface area. After HTT, the layer–layer space among graphite crystallite decreased and the degree of graphitization was improved. The specific capacitance of mesoporous carbons (MoC and ACF) increased, but the specific capacitance of microporous carbon MiC decreased after HTT. At the same time, high temperature treatment could improve the electrical conductivity and decrease the impedance of the electrode remarkably. The improved specific capacitance and the better conductivity of mesoporous carbons could be ascribed to the clear increase of mesopore ratio as well as the expanding and reorganization of crystallite structure.

## Acknowledgements

This work had been performed with financial support from Fund of 863 Project of China (2006AA11A166), Fund of Nature Science Foundation of China (50602046) and Fund of Nature Science Foundation of Shanxi Province (2007011075).

## References

[1] R. Kötz, M. Carlen, Electrochim. Acta 45 (2000) 2483.
[2] P.J. Mahon, C.J. Drummond, Aust. J. Chem. 54 (2001) 473.
[3] A. Nishino, J. Power Sources 60 (1996) 137.
[4] J. Nickerson, Proceedings of the Ninth International Seminar on Double Layer Capacitors and Similar Energy Storage Devices, Deerfield Beach, FL, 1999.
[5] X. Andrieu, Energy Storage Syst. Electron: New Trends Electrochem. Technol. 1 (2000) 521.
[6] E. Frackowiak, F. Béguin, Carbon 39 (2001) 937.
[7] K. Kierzek, E. Frackowiak, G. Lota, G. Gryglewicz, J. Machnikowski, Electrochim. Acta 49 (2004) 515.
[8] A. Alonso, V. Ruiz, C. Blanco, R. Santamarıa, M. Granda, R. Menendez, S.G.E. De Jager, Carbon 44 (2006) 441.
[9] F. Beguin, specially invited report of the 14th International Symposium on Intercalation Compounds, Seoul, 2007.
[10] Z. Qiao, J. Li, N. Zhao, C. Shi, New Carbon Mater. 19 (2004) 236.
[11] V. Ruiz, C. Blanco, E. Raymundo-Pinero, V. Khomenko, F. Beguin, R. Santamarıa, Electrochim. Acta 52 (2007) 4969.
[12] Z. Tang, Y. Song, Y. Tian, L. Liu, Q. Guo, Micropor. Mesopor. Mater. 111 (2008) 48.
[13] J. Liu, K. Gu, Chem. Ind. Forest Prod. 19 (1999) 248.
[14] D. Qu, H. Shi, J. Power Sources 109 (2002) 403.
[15] X. Liu, Y. Yang, H. Liu, W. Ji, C. Zhang, B. Xu, Mater. Lett. 61 (2007) 3916–3919.
[16] M. Endo, T. Maeda, T. Takeda, Y.J. Kim, K. Koshiba, H. Hara, M.S. Dresselhaus, J. Electrochem. Soc. 148 (2001) 910.
[17] Y.R. Nian, H. Teng, J. Electrochem. Soc. 149 (2002) 1008.
[18] K.H. An, W.S. Kim, Y.S. Park, J.M. Moon, D.J. Bae, S.C. Lim, Y.S. Lee, Y.H. Lee, Adv. Funct. Mater. 11 (October (5)) (2001).
[19] Q. Yang, J. Zheng, M. Wang, Ion Exchange Adsorption 15 (1999) 385.